INTERNATIONAL SOCIETY FOR
SOIL MECHANICS AND
GEOTECHNICAL ENGINEERING

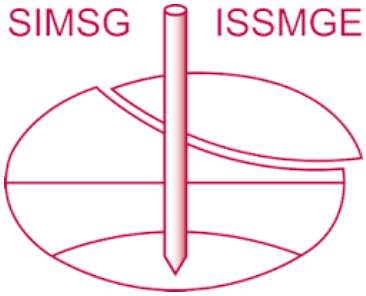

This paper was downloaded from the Online Library of the International Society for Soil Mechanics and Geotechnical Engineering (ISSMGE). The library is available here:

https://www.issmge.org/publications/online-library

This is an open-access database that archives thousands of papers published under the Auspices of the ISSMGE and maintained by the Innovation and Development Committee of ISSMGE.

Calculation method for residual displacement during earthquake for embankment affected by seepage water

Méthode de calcul du déplacement résiduel dû au séisme pour le remblai affecté par l'infiltration d'eau

T. Matsumaru, K. Kojima, M. Tateyama, K. Watanabe
Railway Technical Research Institute, Kokubunji, Japan
& H. Watanabe
Obayashi Corporation, Shizuoka, Japan

ABSTRACT
During the mid Nigata prefecture earthquake in 2004, a lot of railway and road embankments collapsed in mountain regions. It seems that the main reason of these damages was the increase of the degree of water saturation and the water level in embankments caused by the typhoon just before this earthquake. This paper aimed at developing a caluclation method for the residual displacement during earthquake for embankment affected by seepage water. We conducted the shaking table tests of the embankment affected by seepage water and simulation analyses, to confirm the effectiveness of the calculation method, taking into consideration the effect of seepage water and based on Newmark method.

RÉSUMÉ
Lors du Séisme de Chu-etsu dans la préfecture de Niigata en 2004, les remblais des montagnes ont subi des dégâts importants, dont une des causes est sans doute l'augmentation du niveau d'eau et du degré de saturation dans les remblais sous l'influence du typhon qui a immédiatement précédé le séisme. Cette étude a pour objectif l'établissement d'une méthode de calcul du déplacement résiduel dû au séisme des remblais ayant subi l'influence d'une infiltration d'eau. Des essais de secousses des remblais à eau d'infiltration et des calculs numériques ont été effectués, et la pertinence de la méthode de calcul a été étudiée en tenant compte de l'influence de l'eau d'infiltration selon la méthode de Newmark.

Keywords :embankment, seepage water, shaking table test, Newmark method

1 INTRODUCTION

During the Nigata-ken Chuetsu Earthquake which occurred in 2004, a lot of railway and road embankments collapsed in mountainous regions. It appears that the main reason of these damages was the increased degree of water saturation and the water level in the embankments caused by the typhoon just prior to the earthquake. Therefore, the evaluation of the seismic resistance for embankment subjected to seepage water is important.

For example, Ichii (2005) revealed by shaking table tests that the seismic resistance of embankment subjected to rainfall was decreased. Matsuo et. al. (2002) conducted a series of dynamic centrifuge tests on the embankment affected by seepage water. They showed the relationship between the residual displacement and the density of the embankment or the water level, and the effects of countermeasure methods. Okawa et al. (2007) studied the adaptation of calculation methods used for the design of embankment: the circular slip method and Newmark method. However, a few researches previously conducted have focused on evaluating the mechanism of collapse; accordingly, any seismic design method has not been established considering the effect of seepage water.

In this paper, we conducted shaking table tests of the embankment affected by seepage with intention of evaluating the adverse effect of the seepage on seismic resistance. Furthermore, we proposed a calculation method of residual displacement of embankment subjected to seepage water, based on the results of shaking table tests. The efficiency of the method was evaluated by conducting the simulation analyses of the shaking table test.

2 SHAKING TABLE TESTS

2.1 *Conditions of shaking table tests*

Figure 1 shows the experimental model of the embankment. The dimension of the embankment was 60 cm in height and 1: 1.5 in gradient of slope. The material of the embankment was Inagi sand, whose particle density G_s was 2.723; 50% diameter on the grain size diagram D_{50}, 0.134mm; the uniformity coefficient U_c, 9.29; the fine fraction content F_c, 23.6%; and the maximum dry density $\rho_{d\max}$, 1.517 g/cm^3. The embankment was prepared so that the dry density ρ_d would be 1.108g/cm^3 and the water content w was about 13%. The saturated permeability with dry density 1.108 g/cm^3 was 4.8×10^{-3} cm/s, obtained from the permeability test in the laboratory. The dry density of the embankment was much smaller than the maximum dry density, in order to make the seepage easy and to avoid setting the cohesion excessively taking similarity law into consideration. On the other hand, the dry density of the ground was set at 1.365 g/cm^3 (the degree of compaction was 90%) with efficient compaction for avoiding the occurrence of settlement and liquefaction. The measurements included the

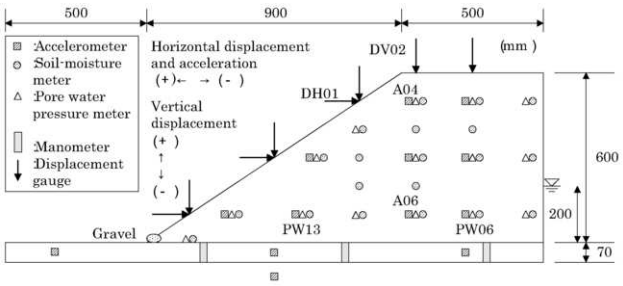

Figure 1. Experimental model of embankment.

© 2009 IOS Press.
doi:10.3233/978-1-60750-031-5-1706

degree of saturation and water level for evaluating water content just before the shaking, and acceleration, excess pore water pressure and displacement for making dynamic behavior of the embankment clear. Furthermore, we photographed reference points in the embankment with a high-speed camera and analyzed the obtained data in order to estimate a deformation mode. We set three manometers in the embankment for measuring the water level.

We poured water into the embankment by maintaining the water level 200 mm in the water tank prepared at the back of the embankment. The shaking was conducted after confirming the rise of water level at the toe of the embankment. We conducted two cases of shaking using two waves, one of them was a sinusoidal wave of 5 Hz and the other was an irregular wave of 5 Hz in predominant frequency based on the wave observed in Hyogoken-Nanbu earthquake in 1995. For both cases, the shaking table test was continued until the embankment collapsed by increasing the maximum acceleration with an increment of about 200 gal. Figure 2 shows the examples of the input motion used in CASE 1 and CASE 2.

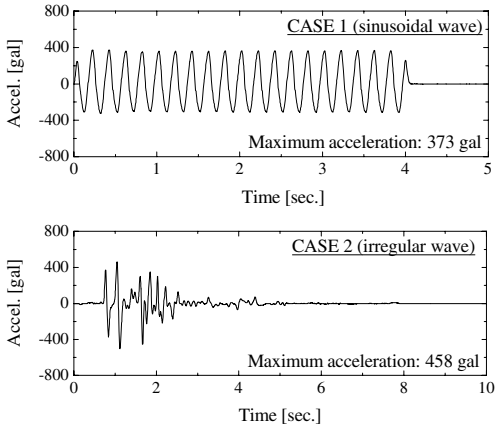

Figure 2. Examples of input acceleration.

2.2 *Results of shaking table tests*

Figure 3 shows the distributions of the degree of saturation and the water level estimated from the measurements of the manometers just before starting the shaking table tests. We showed the result only in CASE 2 because we obtained almost the same results in CASE 1 and CASE 2. The degree of saturation was calculated by using the moisture content measured by the soil-moisture meters. The water line was supposed to be shaped gently from the back of the embankment to the toe, but the region of the degree of saturation S_r=100% was widely spread above the water line. The water content w=13%, which was the water content at the construction of the embankment, corresponds to the degree of saturation S_r=24%. It was revealed that the degree of saturation increased at all positions of soil-moisture meters installation, because of the suction of unsaturated soil.

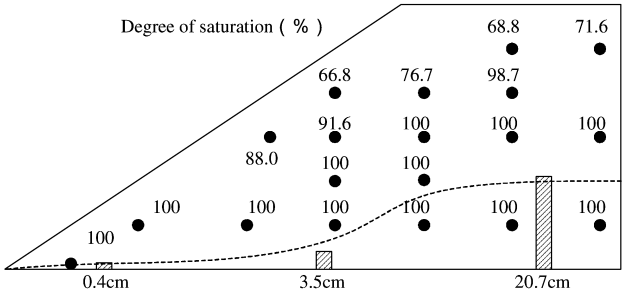

Figure 3. Distributions of degree of saturation and water level.

In CASE 1, the deformation of the embankment did not occur with 187 gal shaking. The acceleration of the input motion was defined as the maximum value in the direction of plus (in the direction of the slope as shown in Fig. 1). However, the embankment was deformed largely by 373 gal shaking, so we finished the series of the shaking. In CASE 2, the deformation did not occur with 208 gal and 354 gal shaking. The embankment started to be deformed with 458 gal shaking and was deformed largely by 546 gal shaking. Photo 1 shows the photograph after the experiment in CASE 2. By the shaking, the top of embankment settled and moved toward the direction of the slope, and a lot of cracks appeared at the top and the slope surface. Furthermore, large strain would occur around the water line, judged from the movement of the reference points.

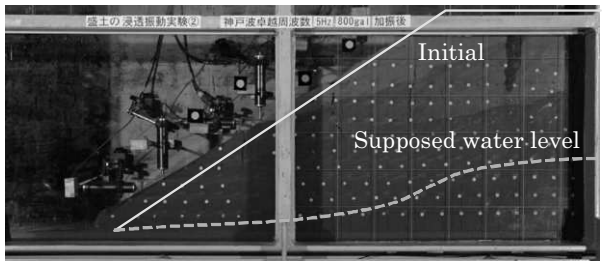

Photo 1. Photograph after shaking in CASE 2.

In order to study the behavior of the embankment during earthquake, we focused on the shakings with 373 gal in CASE 1 and 458 gal in CASE 2. Figure 4 shows the time histories of the responses of acceleration (A04 and A06 in Fig. 1), the excess pore water pressure (E.P.W.P.) (PW06 and PW13) and the displacement (DV02 and DH01). In the time history of the displacement, we showed not only the displacement measured by the displacement gauge but also the displacement obtained from the analysis of the reference points, in case of occurrence of measurement beyond the range of the displacement gauge. The directions were shown in Fig. 1 by sings of plus (+) and minus (-) of acceleration and displacement. The excess pore water pressure was defined as 0 before shaking and the incremental pressure during shaking.

For clarifying the reason of the increase of the excess pore water pressure, we compared the time histories of the displacement and excess pore water pressures. As shown in the time histories of the displacement, both the lateral and horizontal displacement occurred at Time I as shown in Fig. 4, when the first large motion was inputted. On the contrary, the excess pore water pressures at PW06 and PW13 was almost 0 at Time I and increased at Time II, when the maximum amplitude was inputted. This indicated that the excess pore water pressure increased by the occurrence of the negative dilatancy accompanying with the deformation of the embankment.

In the time history of the acceleration at A04, we showed the amplification ratio defined as the ratio of response acceleration to input acceleration. At Time II, the response of the embankment showed the excessive amplification because the amplification ratio was much larger than that at Time I. Later, we studied this reason by relating to the progress of the shear strain in the embankment. Furthermore, it was evident that the response of the acceleration changed from amplification to the damping after Time II because the amplification ratio at Time III was smaller than 1.0. We have two reasons for this phenomenon; the first one was the occurrence of the slip line caused by the deformation of the embankment. This phenomenon was also measured in the shaking table tests without the influence of the seepage of water. The other reason would be the increase of the excess pore water pressure. The time histories in Fig. 4 show that the excess pore water pressure started to increase rapidly at Time II and was maintained at Time III. Moreover, from the time histories in CASE 1, we can understand that the response of the acceleration not only at A04 but also at A06, located at the lower part of the slip line, showed the damping and the shape of the response of the acceleration

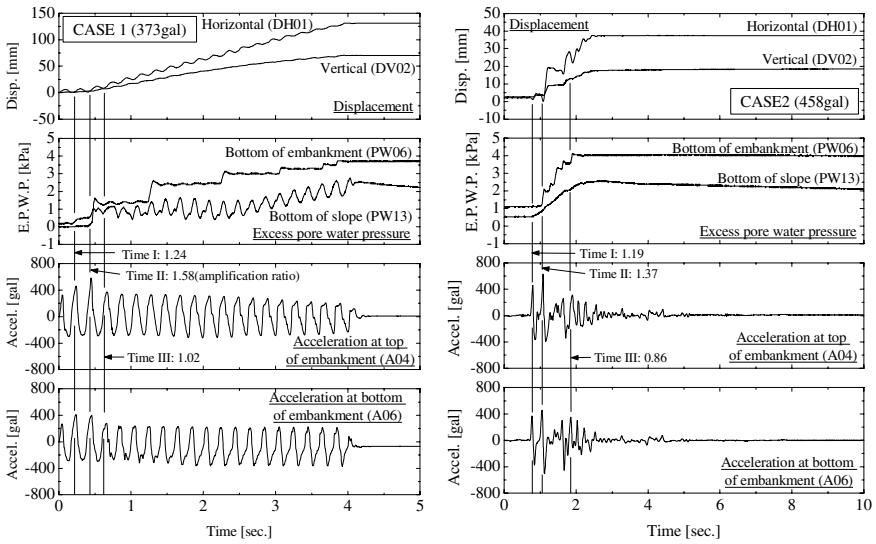

Figure 4. Time histories of acceleration, excess pore water pressure and displacement.

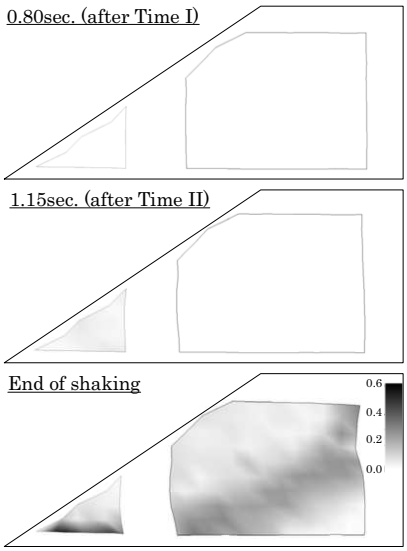

Figure 5. Distributions of maximum shear strain.

was sharper than that of the input motion after Time II (Fig. 2). Therefore, the influence of the cyclic mobility caused by the increase of the excess pore water pressure would appear in the response of the embankment.

In order to research the progress of the collapse of the embankment, we evaluated the distributions of strain in the embankment at each time. Based on the coordinate of the reference points, the strain was calculated by the moving least square method used in meshless method. Figure 5 shows the distributions of the maximum shear strain at 0.80 sec. (just after Time I as shown in Fig. 4), at 1.15 sec. (just after Time II) and after shaking, with 458 gal shaking in CASE 2.

At 0.80 sec. (just after Time I), the maximum shear strain was small, so the response of the embankment would be elastic. On the other hand, at 1.15 sec. (just after Time II), large strain appeared around the toe of embankment. At this time, the stiffness of the embankment would not be decreased because the excess pore water pressure was almost 0. The amplitude of the input motion showed maximum value at this time, so it seems that the main reason of the appearance of the slip surface was the amplitude of the input motion. Furthermore, at this time, the excessive amplification was also observed at the top of the embankment as shown in Fig. 4. The embankment would start to be deformed plastically from this time, so the excess pore water pressure would increase rapidly after this time.

At the time after shaking, the distributions of strain showed circular shape. This suggested that the embankment was deformed with the slip surface of circular shape.

In CASE 1, the photographs of the reference points by the high speed camera became impossible during shaking because the degree of deformation was larger than that in CASE 2. However, the obtained results of image analyses showed the same tendency as the results with 458 gal shaking in CASE 2.

3 CALCULATION OF RESIDUAL DISPLACEMENT DURING EARTHQUAKE

3.1 *Design method of railway embankment against earthquake and rainfall*

In the design standard for Japan railway, the design of embankment against large scale earthquake (L2) is conducted by evaluating the residual displacement during earthquake (R.T.R.I., 2007). For the calculation of the displacement, Newmark method assuming that the slip surface is circular is suitable because of its simplicity.

On the other hand, the design of embankment against rainfall is also important because the stiffness of embankment would be affected by the rainfall. Usually, the stability of embankment is checked by the circular slip method with consideration of the effect of rainfall. The way considering the effect of rainfall is achieved through setting the water level and strength parameters according to the distributions of the degree of saturation. From the triaxial tests on specimens in unsaturated states, it was revealed that the cohesions of the specimens whose degree of saturation was larger than 80% decreased though the cohesions for $S_r < 80\%$ were almost constant (Kojima et al., 2008). With due consideration on this tendency, the cohesions c of soil materials for $S_r < 80\%$, $80 \le S_r < 100\%$ and $S_r = 100\%$ are prepared for the case where conducting triaxial tests is difficult, in the design standard of Japan railway. On the other hand, the internal friction angle is almost constant for all degree of saturation, so the internal friction angle is not distinguished according to the degree of saturation.

3.2 *Calculation of residual displacement during earthquake for embankment affected by seepage water*

From the results of the shaking table tests in the chapter 2, it was revealed that the embankment was deformed with similarity to the shape of circular slip and the excess pore water pressure did not increase when the deformation of the embankment started. So, it would be possible to evaluate the residual displacement during earthquake by Newmark method. In the calculation, it would be important to consider the influence of the increase of the water level and the degree of saturation just before earthquake.

In order to show the validity of the proposed method, we conducted the simulation analyses of the shaking table tests.

3.2.1 *Conditions of calculation*

Though the parameters c and ϕ should be determined from the triaxial tests for the specimens whose densities coincide with those of the embankment and the ground, we did not conduct triaxial tests using the specimens for the densities. Therefore, we have made use of ϕ and c of Inagi sand for the wide range of density by the triaxial tests. Figure 6 shows the relationship between the dry density and the internal friction angle or the cohesion for $S_r < 80\%$ of Inagi sand obtained by the triaxial tests. We applied the least square method to this relationship and obtained ϕ and c for the densities of the embankment and the ground. However, ϕ and c were set at integer. The cohesions for $80 \le S_r < 100\%$ and for $S_r = 100\%$ were set respectively as the half of that for $S_r < 80\%$ and 0, according

to the policy of the design standard of Japan railway. Table 1 shows the determined strength parameters for calculation.

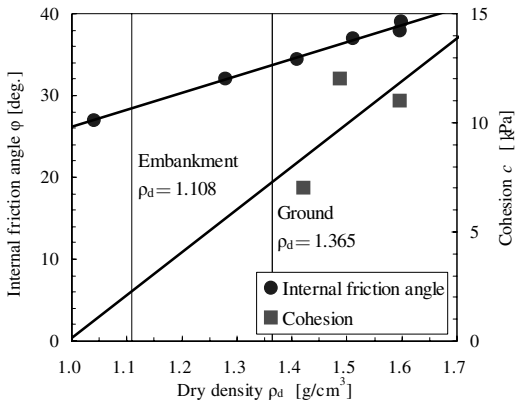

Figure 6. Relationship between density and strength parameters.

Table 1. Determined strength parameters.

	Degree of saturation (%)	Internal friction angle (degree)	Cohesion (kPa)
Embankment	$S_r < 80$	28	2
	$80 \le S_r < 100$		1
	$S_r = 100$		0
Ground	$S_r < 80$	34	7
	$80 \le S_r < 100$		0

The water level and the distribution of the degree of saturation in the embankment were determined by the experimental results as shown in Fig. 3. The strength parameters were determined according to the distributions of the degree of saturation. Furthermore, in this calculation, we did not assume the slip on the slope surface but the circular slip passing through the toe of embankment.

3.2.2 *Results of calculation*

For the comparison, we tried calculating the residual displacement during the earthquake without consideration of the water level and the degree of saturation. In this calculation, the strength parameters only for $S_r < 80\%$ were used. The yielding seismic coefficient was calculated at K_y=0.80. This indicated that the deformation of the embankment did not occur for all of the input motions used in the experiments (Fig. 2), so the calculation did not fit the experiments. On the other hand, we achieved K_y=0.17 by considering the water level and the distributions of the degree of saturation. This indicated that the seismic resistance of the embankment remarkably decreased by the influence of the increase of the water level and the degree of saturation. Figure 7 shows the distributions of the degree of saturation and the circular slip obtained from both calculations. In Fig. 7, the circular slip was also shown without considering the water level and the degree of saturation. From the comparison with the position of the crack (Fig. 3) and the circular slip obtained from the image analyses, we can understand that the calculation considering the water level and the distribution of the degree of saturation indicates the position of the circular slip better.

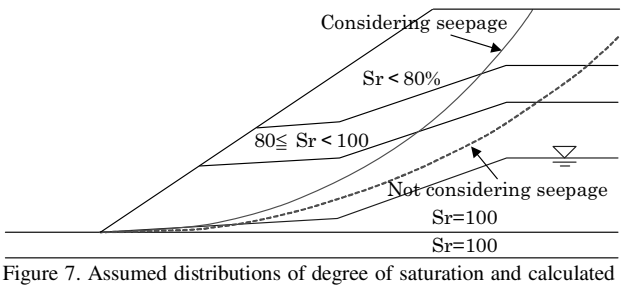

Figure 7. Assumed distributions of degree of saturation and calculated slip surface.

Figure 8 shows the relationship between acceleration of input motion and displacement calculated by using Newmark method. For both cases, the calculated deformations in each step of the shaking coincided with the experimental results, so it seemed to be that the proposed method to consider the water level and the degree of saturation was suitable for the evaluation of the residual displacement.

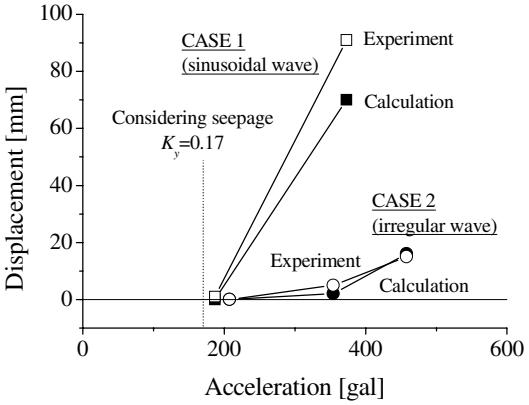

Figure 8. Residual displacement of calculation and experiment.

4 CONCLUSIONS

The purpose of this paper was developing the calculation method for the residual displacement during earthquake for embankment affected by seepage water. We conducted the shaking table tests and the simulation analyses, to confirm the usage of the proposed calculation method. As the results, we achieved the following conclusions:

1. From the shaking table tests, the embankment deformed as the shape of the circular slip. The appearance of the slip surface would be triggered by the amplitude of the input motion. Furthermore, it was found out that the response of the embankment changed from the amplification to the damping because of the progress of the slip surface and the increase of the excess pore water pressure.
2. For the calculation of residual displacement, we proposed the method considering the water level and the degree of saturation in Newmark method. In the simulation analyses of shaking table tests, the calculated displacement using the proposed method almost coincided with the experimental results though the calculation without considering the seepage water could not explain the results of the experiments. Therefore, the validity of the proposed method was proved.

REFERENCES

Ichii, K. 2005. Experimental study on seismic resistance reduction of embankment due to rainfall, Journal of Earthquake Engineering, pp.1-8. (in Japanese)

Kojima, K., Matsumaru, T., Tateyama, M., Isono, J., Koseki, J. and Watanabe, H. 2008. Seismic design method for embankment affected by seepage water using Newmark method, Proceedings of the 40th Japan National Conference of Geotechnical Engineering, pp. 1149-1150. (in Japanese)

Matsuo, O., Saito, Y., Sasaki, T., Kondoh, K. and Sato, T. 2002. Earthquake-induced flow slides of fills and infinite slopes, Soils and Foundations, Vol.42, No.1, pp.89-104.

Okawa, H., Sugita, H., Sasaki, T. and Mizuhashi, M. 2007. Experimental study of evaluation method for seismic stability of mountain road fill, Proceedings of the 62th JSCE Annual Meeting, pp.87-88. (in Japanese)

Railway Technical Research Institute (R.T.R.I.). 2007. Design standards for railway structures and commentary (earth structures).